韓國鑛物學會誌 第1卷 第2號(1988)
J. Miner. Soc. Korea, 1, 104-116 (1988)

Berthierine and Nontronite from Sangdong Tungsten Deposits

상동중석광산에서 산출되는 Berthierine과 Nontronite

Soo Jin Kim(김수진), * Won-Sa Kim(김원사), ** and Se-Won Chang(장세원)*[1]

* Department of Geological Sciences, Seoul National University, Seoul 151-742, Korea
(서울대학교 지질과학과)

** Department of Geology, Chungnam National University, Daejeon 302-764, Korea
(충남대학교 지질학과)

ABSTRACT: Berthierine and Nontronite are firstly identified in the Sangdong tungsten ore deposits. Quantitative and qualitative analyses by EPMA and the studies using X-ray diffraction, transmission electron microscopy, and infrared absorption spectroscopy were done to characterize berthierine and nontronite. The data from berthierine are in good agreement with those from other localities. The structural data of the Sangdong berthierine are consistent with the orthorhombic, pseudo-hexagonal form which is more common in samples with high SiO_2 and low Al_2O_3 content. Geologic features suggest that the Sangdong berthierine is diagenetic in origin. However, nontronite might be a product of hydrothermal alteration after the tungsten mineralization.

요약 : 상동중석광상에서 산출되는 berthierine과 nontronite는 국내에서는 최초로 기재되는 광물로서 전자현미분석기에 의한 정성 및 정량분석, X-선 회절분석, 투과전자현미분석, 적외선흡수분광분석등을 통하여 광물학적 성질을 규명하였다. SiO_2의 함량이 높고 Al_2O_3의 함량이 낮은 것으로 밝혀진 상동산 berthierine의 결정구조는 Brindley에 의하여 연구된 결과인 육방정계와 유사한 형태를 보여주는 사방정계와 일치한다. 상동광상에서 산출되는 berthierine은, 그 산출양상으로 보아, 속성작용에 의하여 생성된 것으로 생각되나 nontronite는 중석광화이후의 열수변질산물로 생각된다.

INTRODUCTION

Berthierine is an iron aluminum 1 : 1 type layer silicate that belongs to the serpentine group minerals. The general formula for berthierine is designated as $Y_6Z_4O_{10}(OH)_8$, where $Y=Fe^{2+}$, Mg^{2+}, Fe^{3+}, Al^{3+}, $Z=Si^{4+}$, Al^{3+}, Fe^{3+} (Bhattacharyya, 1983) or $(Fe^{2+}, Mg^{2+})_{3-x}(Fe^{3+}, Al^{3+})_x(Si_{2-x}Al_x)O_5(OH)_4$ (Brindley, 1982). Nontronite is a dioctahedral mineral of the smectite group, having a general formula, $(M_{x+y})(R^{3+}_{2-y}R^{2+}_y)(Si_{4-x}Al_x)O_{10}(OH)_2$, where $R^{3+}=Fe^{3+}$, Al^{3+}, $R^{2+}=Fe^{2+}, Mg^{2+}$, $M=Na,K,Ca$.

Berthierine and nontronite are the principal components of clays which form the clay bed and the materials filling cracks developed in sideritic rocks. The clays are soft, very fine-grained, and colored green to dark green in hand specimens. Such physical properties might have misled the previous workers to interprete them as a chlorite group mineral. However, detailed mineralogical data including X-ray diffraction, electron microprobe analysis, infrared absorption spectroscopy, and electron microscopy show that they are not chlorite group minerals, instead they are aggregates of berthierine and nontronite.

Although occurrence and formation of bert-

1) Present address : Korea Institute of Energy and Resources, Seoul 152-020, Korea
(한국동력자원연구소 석재산업자원연구실)

hierine and nontronite, the major components of the clays in Sangdong mine, may not be directly related to the genesis of tungsten ores, they are in fact closely associated with tungsten ores and also present in the neighboring rocks. It is therefore believed that the characterization and the nature of the clays are evidently helpful for the better understanding of the tungsten mineralization and wall rock alteration in the Sangdong mine. This study aims to disclose the occurrence, mineralogy, and genesis of berthierine and nontronite found in the Sangdong tungsten mine.

OCCURRENCES

Geological cross sections of the ore bodies in the Sangdong mine is shown in Fig. 1. Berthierine and nontronite, the essential minerals of the clays, occur in (1) the clay bed, (2) the sideritic rocks as oolites, (3) the materials filling the interstices of pseudo-breccia, and (4) the fault clays.

(1) the clay bed: A clay bed occurs extensively as a thin layer and is wholey or partly enclosed by sideritic rocks. Its attitude is in general conformable to the bedding of the neighboring rock units. Clays in the clay bed consist mainly of nontronite and berthierine. In addition, small angular rock fragments and scheelite grains are present in the bed. The fabric of clay bed seen under the microscope reveals that the bed is largely sheared. The clay bed has been altered by hydrothermal process.

(2) sideritic rocks: Sideritic rocks here show well developed stratification resulted from rhy-

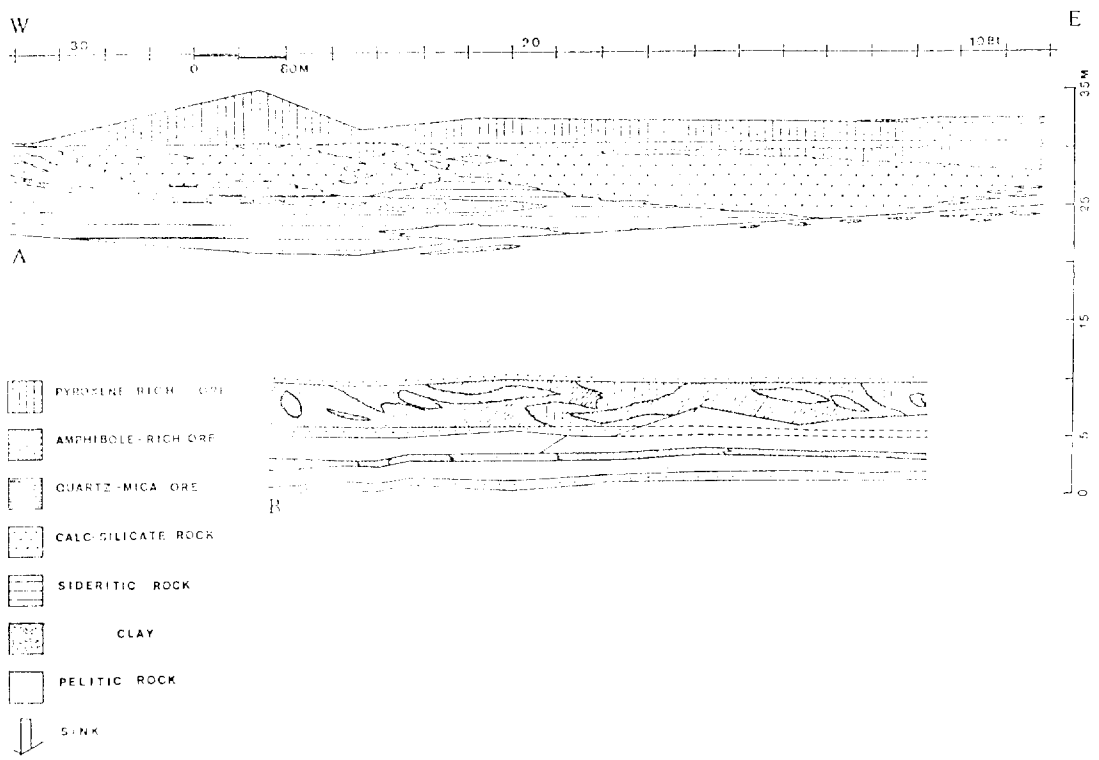

Fig. 1. Gelogical cross sections of the ore bodies in the Sangdong mine.
A: The Hangingwall ore bed from -6 and -5 level.
B: The Main ore bed and the Fl ore bed from -5 level.

thmic layering of siderite, quartz, and berthierine (Fig. 3-2). Oolitic structure is frequently observed in the sideritic rocks (Fig. 3-1). The oolites are found to consist essentially of berthierine together with very small amount of quartz and fluorite. The brownish sideritic rocks become greenish as the content of berthierine increases.

(3) matrix of pseudo-breccia: Breccia-like structure is well developed in the pyroxene-rich and amphibole-rich skarn zones, and even in the sideritic rocks. In places, such structure is relatively readily observed on the surface of sideritic rocks primarily due to marked color contrast between the fragments and surrounding matrix. However, it is rather difficult to discern the structure on the dark-colored skarns because the color contrast between the materials is not so conspicuous. The breccia-like structure is assumed to have been formed by hydrothermal replacement of the skarns and sideritic rocks. Berthierine and nontronite occur abundantly in the matrix that fills the interstices of the rock fragments. They occur along the outer rims of the rock fragments as well.

(4) fault clay: Fault clays are found along the faults. The clay occurring in the pelitic rocks consists of biotite, berthierine, nontronite, quartz, and fluorite, whereas it in the quartz-mica rocks consists of quartz, kaolinite, muscovite, nontronite, and scheelite. Berthierine is not observed in the latter.

Minerals and their abundance are schematically illustrated in Table 1.

ANALYTICAL METHODS

A routine polarizing microscopic observation was made for the thin sections prepared. A Philips model SEM 505 and a JEOL model JCXA-733 Superprobe, both are equipped with energy dispersive spectrum analyser, were used for scanning electron microscopic observations and quantitative chemical analysis. The quantitative analysis was performed under the operating condition of 15kV and 10nA with a beam

Table 1. Minerals and their abundance in the rocks near ore bodies.

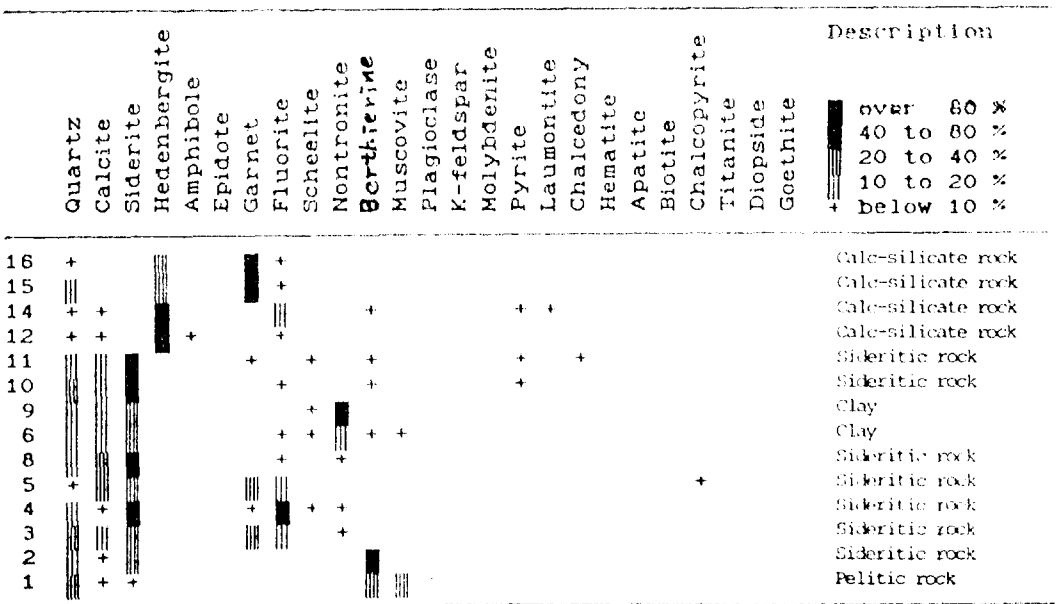

size of 5μ. H_2O was determined by thermal gravimetric analysis.

X-ray powder diffraction work was carried out with a JEOL model JDX-5P X-ray diffractometer. X-ray powder diffractograms were obtained with a scanning speed of the goniometer of 1° (2θ) per minute, using filtered CoK_α or CuK_α radiations. All the runs were operated at 40kV and 40mA. The X-ray powder patterns were indexed and subsequently refined by a least-squares method using Applemann-Evans computer program (Applemann and Evans, 1973).

Electron-optical studies were performed with a JEOL model JEM 120C transmission electron microscope. For this purpose, hand-picked berthierine samples were finely ground in agate mortar and washed with acetone in ultrasonic cleaner. The suspended particles were taken with carbon-coated copper grits covered with collodian films. Bright field images and selected area electron diffraction patterns were taken under the operation condition of 120kV and a focal length of 135cm.

Infrared absorption spectrum was obtained with a Perkin-Elmer model 283B spectrometer on approximately 3mg of powdered sample dispersed in KBr pellets for the range of 4,000 to 300cm^{-1}. The spectrum was initially calibrated against polystyrene film.

RESULTS AND DISCUSSION

Chemical Compositions

The chemical composition of berthierine obtained in this study is shown in Table 2. All iron is treated as ferrous state since microprobe analysis cannot determine the oxidation state of it. Si, Al, Fe, and Mg are the major elements with Mn, Ti, Cr, Ca, and Na minor elements. Of these cations Fe, Mg, Al, Mn, Ti, Cr

Table 2. Chemical analyses and structural formulas of berthierine.

	1	2	3	4	5	6
SiO_2	27.87	19.08	21.26	26.24	26.9	25.5
Al_2O_3	15.21	26.88	23.61	22.17	18.4	14.9
Fe_2O_3	—	4.29	5.08	6.62	—	—
FeO	40.68	34.52	34.62	32.54	36.8	35.6
MgO	3.72	1.55	2.92	1.58	8.15	5.6
MnO	0.13	—	—	0.035	—	1.0
CaO	0.24	—	—	—	—	—
TiO_2	0.01	—	—	—	—	—
Cr_2O_3	0.01	—	—	—	—	—
Na_2O	0.01	—	—	—	—	—
K_2O	—	—	—	—	—	—
H_2O	12.02	11.18	12.51	10.81	9.58	17.4
Σ	99.90	99.25	100.00	100.00	99.83	100.0
Si	1.589	1.097	1.207	1.427	1.457	1.535
Al(IV)	0.411	0.903	0.793	0.573	0.543	0.465
Al(VI)	0.612	0.919	0.787	0.848	0.631	0.592
Fe^{3+}	—	0.186	0.216	0.271	—	—
Fe^{2+}	1.948	1.661	1.644	1.480	1.667	1.792
Mg	0.316	0.133	0.247	0.128	0.658	0.503
Ca	0.014	—	—	—	—	—
Mn	0.007	—	—	0.002	—	0.051
Ti	0.0005	—	—	—	—	—
Cr	0.0005	—	—	—	—	—
Na	0.001	—	—	—	—	—
□	0.100	0.101	0.106	0.271	0.044	0.062
O	—	5.000	5.000	5.038	5.268	5.000
OH	4.000	4.000	4.000	3.924	3.464	4.000
H_2O	0.147	0.147	0.371	—	—	1.496
M:Or*	Or	M>Or	M>Or	Or	—	Or

1. This study. Sample from Sangdong, Korea.
2. Klekl(1979). Sample from Belgorod District, Kursk, USSR. TiO_2 1.44% not included. No recorded impurities.
3. Yershora et al.(1976). Sample from Voronezh anticline, Kursk, USSR. Total H_2O is reported.
4. Thurrell et al.(1970). Sample from Weald clay. After authors corrections for 11.57% impurities.
5. Floran and Papike(1975). Sample from Gunflint Iron Formation. All iron reported as FeO. CaO 0.05%, K_2O 0.12% omitted. H_2O taken as difference from 100%.
6. Deudon(1955). Sample from Sainte-Barbe. Corrected analysis given by Deudon: total impurities 65.1%.

* M: Or signifies ratio of M(monoclinic) to Or (orthorhombic) form.

are considered to occupy the octahedral positions, whereas Si and Al the tetrahedral sites of the mineral. The existence of Ca, Na, and K in berthierines was also recognized by earlier workers including Brindley(1951), Floran and Papike(1975). Brindley(1982) who recently reviewed chemical compositions of berthierine from various sources considered them to have been attributed to impurities by stating in his article that such cations cannot enter octahedral positions. Based on the Pauling's rules, we calculate the radius ratio for individual cations, such as Ca, Na, and K with respect to oxygen anion. The result shows 0.70, 0.69, and 0.95 for the Ca, Na, and K cations, respectively, indicating that Ca and Na have octahedral coordination and K cubic coordination. Therefore, Ca and Na ions are believed to enter the octahedral sites substituting Fe, Mg, Al ions. Small amounts of Ca and Na measured in some berthierine analyses could arise from pure berthierine and are not necessarily attributed to impurities. Calculation of structural formula, on the basis of present chemical data, indicates that tetrahedral sites not filled by all Si are filled by Al of 0.411 atomic moles. The remaining cations are considered to occupy the octahedral positions and the deficit from a total of three is represented as □ in the following formula: $(R_a^{2+}\ R_b^{3+}\ \square_c)\ (Si_{2-x}Al_x)O_5(OH)_4$, given to berthierine by Brindley(1982), where R^{2+}, R^{3+} are cations occupying octahedral positions, □ possible vacant octahedral positions, and $a+b+c=3$. The R^{3+} octahedral cations exceed the Al^{3+} tetrahedral cations and electrical neutrality of the layer is achieved by vacant octahedral site. We could calculate the deficit of 0.10 in the octahedral sites. If R^{3+} (0.61) is plotted against Al^{3+} (0.41), for this berthierine, on the diagram devised by Brindley(1982), it lies near on a line passing through the origin (Fig. 2),

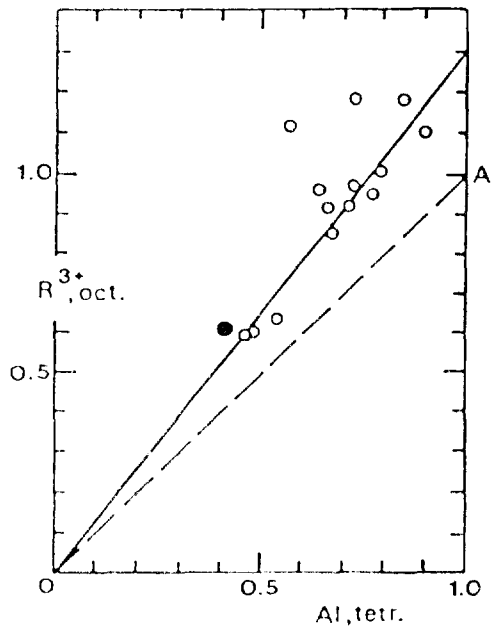

Fig. 2. ΣR^{3+}(octahedral) vs. Al^{3+}(tetrahedral). Point A corresponds to composition of amesite when $R^{3+}=Al^{3+}$. Dashed line corresponds to R^{3+}(oct.)=Al^{3+}(tet.)=Al^{3+}(tet.). Circles=berthierines from various sources. Solid dot=Sangdong berthierine. Full line has slope=1.30. (After Brindley, 1982).

suggesting good chemical agreement with berthierine from other sources. Examples of chemical analyses of berthierine are listed (Table 2) in order to compare with that from Sangdong mine. Berthierine differs from lizardite ($Mg_3Si_2O_5(OH)_4$), a magnesium serpentine, in having Fe^{2+} octahedral cations and an excess of R^{3+} ions, namely Al^{3+}, with compensating vacant sites.

The EDS analysis (Fig. 3-10) made on the nontronite specimen shows that Si, Fe, Ca, Al, and Mg are the elements of it. Accurate quantitative analysis was not attempted due to difficulty in separating pure nontronite sample from the clay samples.

X-ray Diffraction Data

Brindley(1951) reported berthierine to have

hexagonal and monoclinic structures. He also found that X-ray powder patterns of berthierine vary considerably which might be due to the presence of both orthorhombic and monoclinic stacking of layers. The X-ray powder diffraction data of berthierine (Brindley, 1951) were produced in fact by mixture of the two polytypes. Brindley and Youell(1953) later reported the X-ray powder data of hexagonal form and indexed the reflections on the basis of orthorhombic cell with a=5.415, b=9.379, c=7.114Å (Table 3). X-ray powder patterns of berthierine (Table 3) obtained in this study compare reasonably well with those of hexagonal form reported by Brindley and Youell(1953). They can be successfully indexed on the basis of the

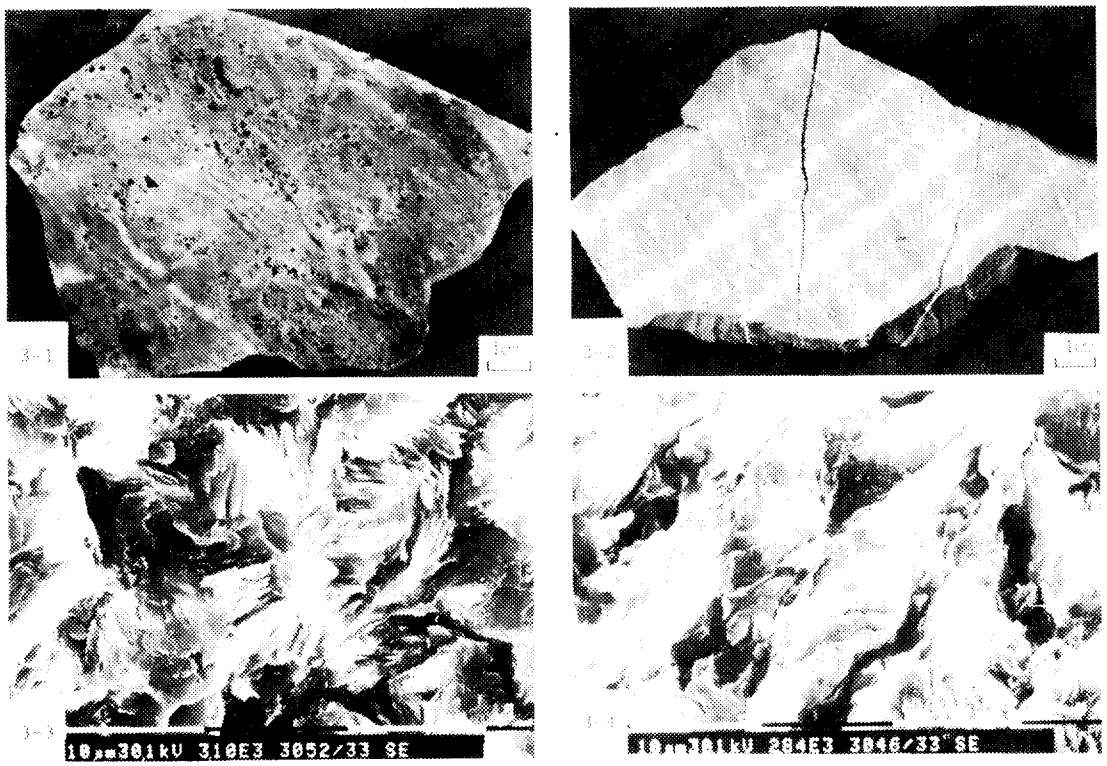

Fig. 3. Microphotographs for berthierine and nontronite.

1. The hand specimen of the berthierine-bearing siderostone from the southwestern part of the main ore bed. The black colored spots are berthierine.
2. Hand specimen of siderostone found in the east part of the main ore bed. It shows well-developed laminations.
3. SEM photograph of berthierine showing flaky habit and platy shape.
4. SEM photograph of berthierine and nontronite showing the preferred orientation.
5. Selected area diffraction pattern of berthierine under TEM. Spot pattern shows orthorhombic symmetry.
6. Bright field amage of berthierine under TEM. ×40,000.
7. Energy dispersive spectrum of berthierine. Fe, Si, and Al peaks are intensely revealed.
8. Selected area diffraction pattern of nontronite under TEM. Spots and ring patterns show orthorhombic structure.
9. Bright field image of nontronite under TEM. ×40,000.
10. Energy dispersive spectrum of nontronite showing Fe, Ca, Al, Mg, Si lines. It indicates the interlayer cation to be Ca.

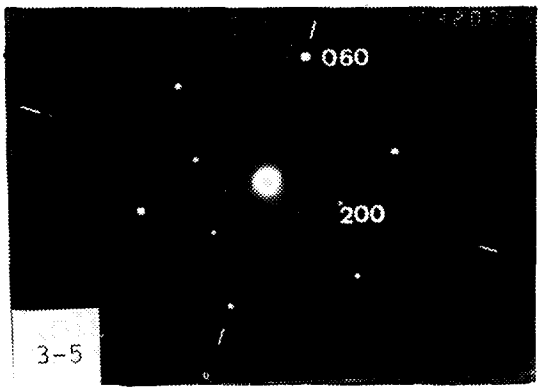

3-5

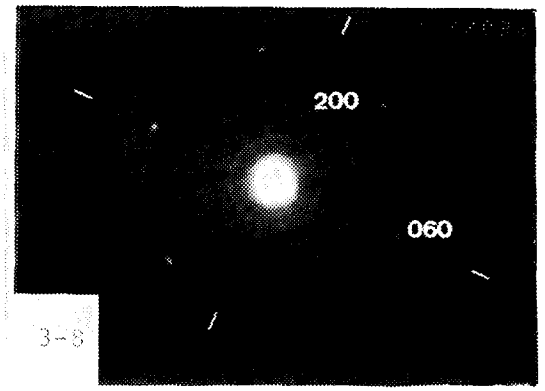

3-8

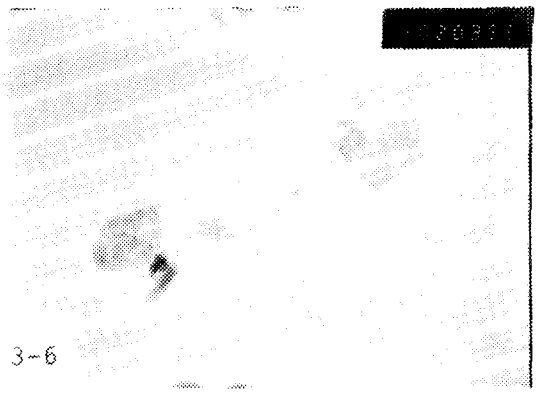
3-6

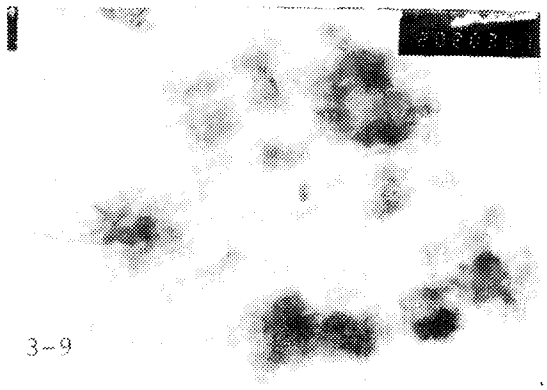
3-9

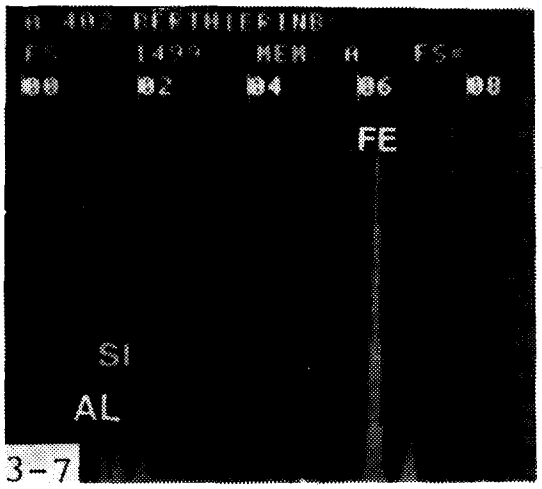

3-7

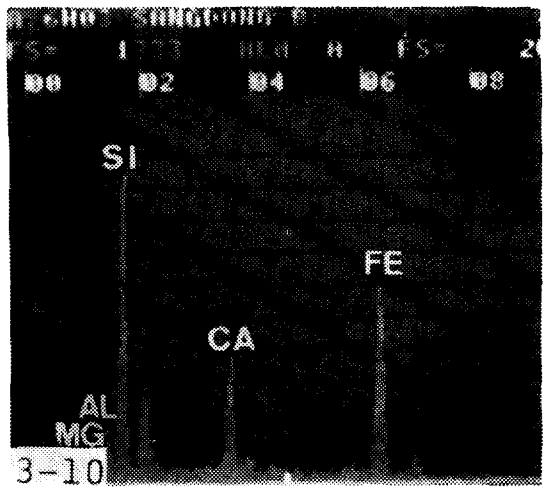

3-10

Table 3. X-ray powder diffraction data of berthierine.

Berthierine[1] a =5.371 b =9.312 c =7.057Å				Berthierine[2] a =5.415 b =9.379 c =7.114Å	
hkl	$d_{obs.}$	$d_{cal.}$	I	$d_{obs.}$	I
001	7.09	7.05	v s	7.12	100
02*	—	—	—	4.68	50
110	4.56	4.65	w	—	—
——	—	—	—	4.30	20
021	—	—	—	3.93	30
022	3.53	3.52	s	3.55	100
——	—	—	—	3.07	20
200	2.673	2.686	w	3.71	50
201	2.502	2.501	s	2.53	100
202	2.131	2.137	w	2.15	70
240, 203	1.760	1.759	w	1.779	60
060	1.551	1.552	s	1.563	70
061	1.515	1.516	m	1.526	50
204	1.473	1.475	w	1.481	60
062	1.422	1.421	w	1.433	40
005, 044	—	—	—	1.416	10
401	1.320	1.319	w	1.327	40
063	1.293	1.295	v w	—	—
402	1.256	1.255	w	—	—
065	1.045	1.044	w	—	—
007	1.008	1.008	w	—	—

1. This study. CoK_α radiation. s: strong, m: medium, w: weak.
2. PDF 7-339 (Brindley and Youell, 1953). CoK_α radiation.

orthorhombic cell as shown in Table 3. The refined cell parameters of berthierine, calculated by a least-squares method, are a=5.371, b=9.312, c=7.057Å, showing good agreement with those given by Brindley and Youell(1953). The same X-ray powder data may also be indexed on hexagonal axes, as illustrated in Table 4, and the cell-dimensions refined by a least squares method are a=5.374, c=7057Å, and V=176.51Å^3. It is noted that the present X-ray powder data are not comparable to those of monoclinic form reported by Brindley(1951).

Table 4. X-ray powder diffraction data of berthierine and lizardite.

Berthierine[1] Hexagonal a =5.374 c =7.05Å				Lizardite[2] Hexagonal a =5.340 c =7.100Å	
hkl	$d_{obs.}$	$d_{cal.}$	I	$d_{obs.}$	I
001	7.09	7.05	v s	7.10	82
100	4.56	4.65	—	4.63	42
101	—	—	—	3.88	46
002	3.53	3.52	s	3.55	57
102	—	—	—	2.816	15
110	2.673	2.687	w	2.670	5
111	2.502	2.511	s	2.499	100
003	—	—	—	2.367	6
200	—	—	—	2.312	1
201	—	—	—	2.199	3
112	2.131	2.138	w	2.133	45
103	—	—	—	2.107	5
202	—	—	—	1.938	5
004	—	—	—	1.775	1
113	—	—	—	1.771	32
210	1.760	1.759	w	—	—
120	—	—	—	1.748	4
121	—	—	—	1.697	7
203	—	—	—	1.654	4
122	—	—	—	1.568	5
300	1.551	1.551	s	1.542	26
301	1.515	1.515	m	1.506	11
114	1.473	1.475	w	1.478	28
302	1.422	1.420	w	—	—
005	—	—	—	1.420	2
302	—	—	—	1.414	6
204	—	—	—	1.408	3
123	—	—	—	1.406	2
220	—	—	—	1.335	3
221	1.320	1.320	w	1.312	15
303	1.293	1.295	v w	1.292	4
130	—	—	—	1.283	1
115	—	—	—	1.254	8
222	1.256	1.256	w	1.250	4
124	—	—	—	1.245	1
205	—	—	—	1.210	2
006	—	—	—	1.183	1
305	1.045	1.044	w	—	—
007	1.008	1.008	w	—	—

1. This study. CoK_α radiation. s: strong, m: medium, w: weak
2. PDF 22-1161 (Bailey, 1969). $Mg_3Si_2O_5(OH)_4$.

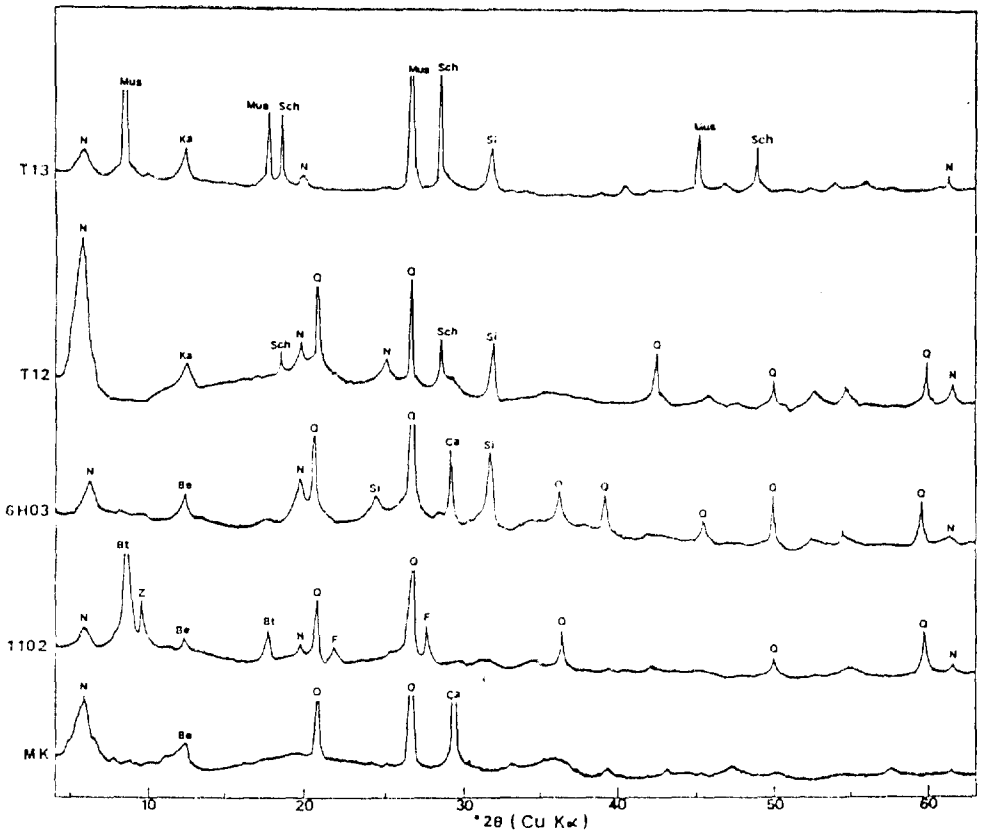

Fig. 4. X-ray diffraction diagrams for bulk samples of clays. Be: Berthierine, Bt: Biotite, Ca: Calcite, F: Feldspar, Ka: Kaolinite, Mus: Muscovite, N: Nontronite, Q: Quartz, Sch: Scheelite, Si: Siderite, Z: Zeolite

MK: Clays in the Hangingwall shear zone. It is composed of nontronite, berthierine, quartz and calcite.

1102: Fault clay in the pelitic rock. It is composed of biotite, berthierine, nontronite, quartz, and fluorite.

6H03: Clays filling the fractures in the sideritic rock. It is composed of nontronite, quartz, calcite, siderite, and minor scheelite and berthierine.

T12: Fault clay in the quartz-mica ore from the Main ore bed. It is greenish in color and mainly composed of nontronite, quartz, scheelite, siderite, and kaolinite.

T13: Fault clay in the quartz-mica ore from the Main ore bed. It cuts the ore obliquely. It is gray in color and composed of muscovite, scheelite, and kaolinite with minor nortronite.

Good correspondence of X-ray powder data between the hexagonal berthierine and hexagonal lizardite(Table 4) may indicate structural identity, supporting the fact that berthierine is ferroan aluminian analogue of lizardite. However, it should be pointed out that lizardite has been reported to have at least 3 more polytypes besides the hexagonal form (Bailey, 1969), i.e., monoclinic (Rucklidge and Zussman, 1965), triclinic (Brindley and Knorring, 1954), orthorhombic(Gillery, 1959). The X-ray powder data of monoclinic berthierine does not agree with those of lizardite of any symmetry. Therefore, the statement that berthierine is ferroan aluminum analogue of lizardite is true only for the two minerals of hexagonal symm-

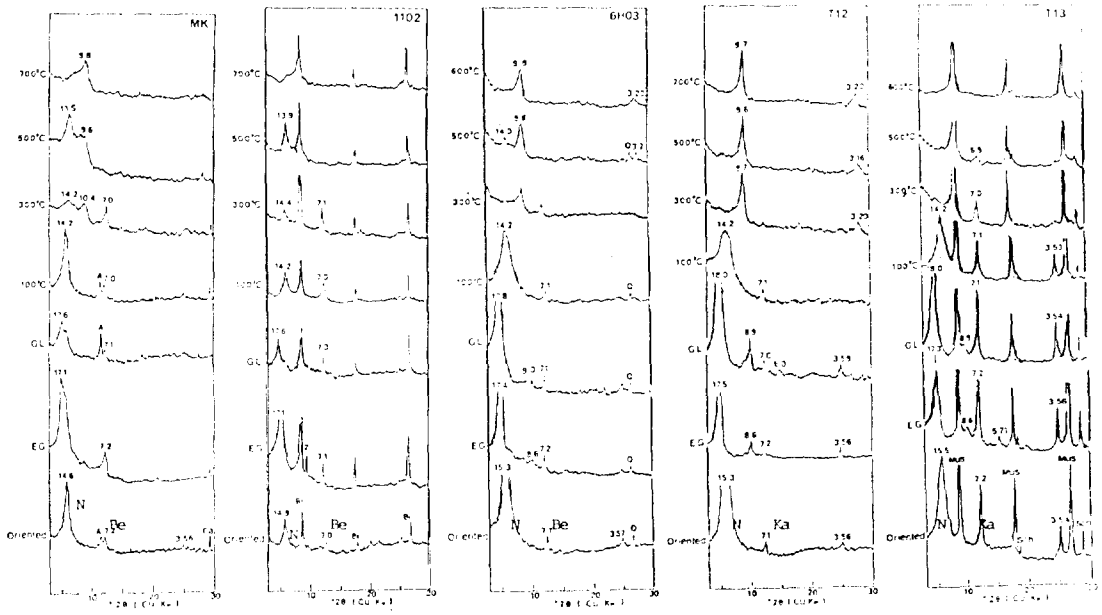

Fig. 5. X-ray diffraction diagrams for clays.
A: Apophyllite, Ca: Calcite, Bt: Biotite, Z: Zeolite, Q: Quartz, Mus: Muscovite, Sch: Scheelite, N: Nontronite, Be: Berthierine, Ka: Kaolinite.

etry. The structure of Sangdong berthierine, characterized by high SiO_2 and low Al_2O_3 contents, is consistent with the observation of Brindley(1982) that the monoclinic form of berthierine is more common in samples with low SiO_2 and high Al_2O_3 contents, while the orthorhombic, pseudo-hexagonal form is more com mon in samples with high SiO_2 and low Al_2O_3 contents,

X-ray powder diffractograms for clay samples containing berthierine as one of the components are illustrated in Fig. 4. The same clay samples were treated with glycerol and ethylene glycol, and heated at selected temperatures to see any structural variations when X-rayed. As shown in Fig. 5, the basal spacing of 7.0~7.2Å for berthierine disappears sharply at 500°C and a long basal spacing of 13.5~14.0Å newly generates. It has been reported to be a characteristic phenomenon observed in all serpentine group minerals and is considered to be due to dehydroxylation (Weaver and Pollard, 1975; Brindley and Chang, 1974; Brindly and Wan, 1975; Maksimovic and Bish, 1978).

X-ray powder data of single-phase nontronite could not be obtained due to failure in getting pure material enough to do X-rays by a powder goniometer method. Systematic X-ray diffraction analyses were performed for nontronite-bearing clays (Fig. 5). Basal spacings of nontronite increases from 14.6~15.5Å to 17.1~17.4Å by ethylene glycolation at 65°C and to 17.6~18.0Å by glycerolation at 110°C. The 14.6~15.5Å basal spacing of nontronite collapses after heat treatment at 300°, 500°, and 700°C and new 9.7~9.9Å and 3.20Å peaks show up.

Scanning and Transmission Electron Microscopy

SEM studies show that berthierine in siderostone from the main ore bed occurs as aggreg-

ates of flaky and platy crystals (Fig. 3-3). Berthierine found in the shear zone occurs as curved flakes and shows a preferred orientation (Fig. 3-4). Transmission electron micrograph (Fig. 3-6) shows that berthierine crystals occur in pseudo-hexagonal(?) form and also elongated lath-like shape. Energy dispersive spectrum (Fig. 3-7) reveals Fe, Si, Al in berthierine. Selected area electron diffraction pattern of berthierine (Fig. 3-5) with (hk0) normal to the electron beam shows sharp spots with $h+k=2n$, suggesting orthorhombic symmetry of the mineral.

Nontronite occurs closely with berthierine in the clays within the shear zone and shows preferred orientation (Fig. 3-4). The selected area electron diffraction pattern of (hk0) plane shows spots of (020), (110), (200), (130), (330), and (060) and also ring patterns superimposed on them (Fig. 3-8).

Infrared Absorption Spectral Data

Infrared absorption spectrum of berthierine (Fig. 6) shows absorption bands at 3564, 3454, 3434, and 1,633cm^{-1}. In the same figure, absorption bands in nontronite occur at 3543, 3434, 2334, 1642, 1008, 835, 710, 655, 450, 350, and 308cm^{-1}. The absorption band at 2334cm^{-1} in nontronite may be due to crystallization water located in different site symmetry of water molecules from berthierine.

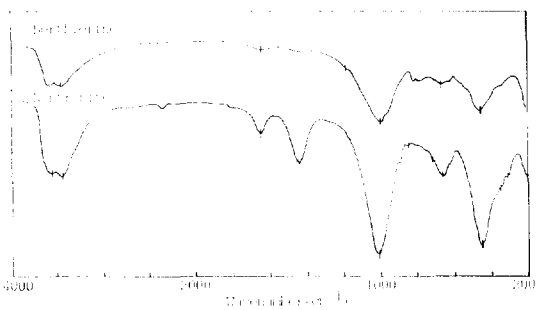

Fig. 6. Infrared absorption spectra for berthierine and nontronite. C: Absorption bands due to calcite.

Origin

Theories on the formation of bertierine are generally divided between the possibility of primary chemical precipitation and of diagenetic replacement of the pre-existing materials in the sediments.

It has been demostrated that direct precipitation of ferrous minerals such as berthierine from shallow, well-oxygenated surface waters is improbable (Curtis and Spears, 1968; Crerar et al., 1979), in the light of fluctuating Eh, pH and solution composition needed to the precipitation of ferric oxide and ferrous silicates. On the other hand, most of the field and laboratory observations suggest diagenetic origin for the berthierine formation, which includes (1) dissolution of argillaceous sediments and reprecipitation as berthierine (Sokolova, 1969), (2) crystallization from amorphous SiO_2, Al $(OH)_3$, $Fe(OH)_3$ precipitates under reducing conditions (Caillere and Henin, 1960; Bubenicek, 1969; Harder, 1978), (3) replacement of calcareous oolites (Kimberly, 1979, 1980), and (4) transformation of detrital kaolinite (Karpov et al., 1967; Schellmann, 1969; Velde, 1977; Iijima and Matsumoto, 1982).

Battacharyya(1983) reported that berthierine in ironstone is essentially diagenetic in origin and is genetically related to a detrital precursor, kaolinite, suggesting the following reactions for kaolinite-berthierine transformation:

$$\underset{\text{(kaolinite)}}{Al_4Si_4O_{10}(OH)_8} + 3Fe^{2+} \rightarrow \underset{\text{(protoberthierine)}}{Fe_3Al_2Si_4O_{10}(OH)_8} + 2Al^{3+} \quad (1)$$

$$\underset{\text{(protoberthierine)}}{Fe_3^{2+}Al_2Si_4O_{10}(OH)_8} + Fe^{2+} + 2Fe^{3+} \rightarrow \underset{\text{(berthierine)}}{Fe_4^{2+}\,Fe_2^{3+}Al_2Si_{12}O_{10}(OH)_4} + 2Si^{4+} \quad (2)$$

Geologic features, such as lamination and

oolites, observed within the sideritic rocks suggest that oolites had already formed prior to the formation as sideritic rocks with oolitic structure. Berthierine-oolites in the sideritic rocks are believed to be diagenetic in origin and they might have been formed from unknown precursors, possibly including amorphous SiO_2-$Al(OH)_3$-$Fe(OH)_3$ precipitates.

Berthierine in the clay bed is believed to be diagenetic in origin as well. The precursor from which berthierine formed is presently unknown but noncrystalline SiO_2-$Fe(OH)_3$-$Al(OH)_3$ precipitates or kaolinite assumed to exist within the original bed would be highly probable for it.

Nontronite in the clay bed, matrix of pseudo-breccia and fault clay is considered to be alteration products of hydrothermal activity of post-tungsten mineralization. Berthierine associated with nontronite in pseudo-breccia is assumed to be the mobilized product from the clay bed at the time of hydrothermal activity.

Acknowledgements: This research was supported by the Basic Science Research Fund (1987) from the Ministry of Education, Korea.

REFERENCES

Appleman, D.E., and Evans, H.T., Jr. (1973) Job 9214: Indexing and least squares refinement of powder diffraction data. U.S. National Technical Information Service, Document PB2-16188.

Baily, S.W. (1969) Polytypism of trioctahedral 1:1 layer silicates. Clays Clay Miner., 17, 355-371.

Bailey, S.W.(1980) Structures of layer silicates: In G.W. Brindley and G. Brown, (eds.), Crystal Structures of Clay Minerals and Their X-Ray Identification. Mineralogical Society, London, 1-123.

Battacharyya, D.P. (1983) Origin of berthierine in ironstone. Clays Clay Miner., 31, 173-182.

Brindley, G.W.(1951) The crystal structures of some chamosite minreals. Mineral. Mag., 29, 502-525.

Brindley, G.W.(1982) Chemical compositions of berthierine-a review. Clays Clay Miner., 30, 153-155.

Brindley, G.W. and Youell, R.F.(1953) Ferrous chamosite and ferric chamosite. Miner. Mag., 30, 57-70.

Brindley, G.W. and Von Knorring, O. (1954) A new variety of antigorite (ortho-antigorite) from Unst, Shetland Islands. Am. Miner., 39, 794-804.

Brindley, G.W. and Chang, T.S.(1974) Development of long basal spacings in chlorites by thermal treatment. Am. Miner., 59, 152-158.

Brindley, G.W. and Wan, H.M. (1975) Compositions, structures, and thermal behavior of nickel-containing minerals in the lizardite-nepouite series. Am. Miner., 60, 863-871.

Bubenicek, L.(1971) Geologie du gisement de fer de Lorrain. Carte Recherches Pau, Soc. Nat. Petroles d'Aquitaine Bull., 5, 223-320.

Caillere, S. and Henin, S.(1960) Propriete des ions et conditions des synthese des mineraux argileux. Le Cas du fer Ged. Int. Cong. Norden, 24, 73-79.

Crerar, D.A., Knox, G.W., and Means, J.L. (1979) Bio-chemistry of bog iron in southern New Jersey. Chem. Geol., 24, 111-135.

Curtis, C.D. and Spears, D.A.(1968) The formation of sedimentary iron minerals. Econ. Geol., 63, 257-270.

Deudon, M. (1955) La chamosite orthorhombique du minerai de Sainte-Barbe, couche grise. Bull. Soc. Fr. Miner. Cristallogr., 78, 475-480.

Floran, R.J. and Papike, J.J.(1975) Petrology

of the low-grade rocks of the Gunflint iron-formation, Ontario-Minnesota. Bull. Geol. Soc. Amer., 86, 1169-1190.

Gillery, F.H. (1959) The X-ray study of synthetic Mg-Al serpentines and chlorites. Am. Miner., 44, 143-152.

Harder, H.(1978) Synthesis of iron layer silicate minerals under natural conditions. Clays Clay Miner., 26, 65-72.

Iijima, A. and Matsumoto, R.,(1982) Berthierine and chamosite in coal measures of Japan. Clays Clay Miner., 30, 264-274.

Karpov, P.A., Losev, A.L., and Shilin, A.V. (1967) Mineralogy and condition of Devonian oolitic iron ore formation on the eastern slope of Voronezh anteclise. Lithology and Mineral Resources, 321-330.

Kimberley, M.M.(1979) Origin of oolitic iron formation. Jour. Sed. Petrol., 75, 97-106.

Kimberley, M.M.(1980) Paz de Rio oolitic inland sea iron formation. Econ. Geol., 75, 97-106.

Klekl, L.V. (1979) Regularities of chamosite distribution in bauxites of the Belgord District of the Kursk magnetic anomaly. Lithol. Miner. Resour. Engl. Transl., 14, 377-382.

Maksimovci, Z. and Bish, D.L.(1978) Brindleyite, a nickel-rich alminous serpentine mineral analogous to berthierine: Am. Miner., 63, 484-489.

Rucklidge, J.C. and Zussman, J. (1965) The crystal structure of the serpentine mineral, lizardite $Mg_3Si_2O_5(OH)_4$. Acta Crystallogr., 19, 381-389.

Schellman, W. (1969) Die Bildungsbedingungen sedimentärer chamosit und Hämatit-Eisenerze am Beispiel der Lagerstätte Echte. N. Jb. Miner. Abh., 111, 1-31.

Thurrel, R.G., Sergeant, G.A., and Young, B.R. (1970) Chamosite in Weald Clay from Horsham, Sussex. Inst. Geol. Sci., HMSO, Rept. 70/7, 7pp.

Velde, B. (1677) Clays and Clay Minerals in Natural and Synthetic Systems. Elsevier Sci. Pub. Co. Amsterdam.

Weaver, C.E. and Pollard, L.D. (1973) The Chemistry of Clay Minerals. Elsevier Sci. Pub. Co. Amsterdam.

Yershova, Z.P., Nikitina, A.P., Perfil'ev, Yu. D., and Babeshkin, A.M. (1976) Study of chamosites by gamma-reasonance (Mössbauer) spectroscopy: In Proc. Int. Clay Conf., Mexico City, 1975, S.W. Baily, ed., Applied Publishing, Wilmette, Illinois, 211-219.